



Structural, Morphological And Optical Properties Of Nanocrystalline $\text{PbTe}_{100-x}\text{Se}_x$ Thin Films

^{1,2*} L. Kungumadevi, ² R. Sathyamoorthy

¹ Department of Physics, ² PG and Research Department of Physics,

¹ Mother Teresa Women's University, ² Kongunadu Arts and Science College,

¹ Kodaikanal, Tamil nadu – 624 101, India. ² Coimbatore, Tamil nadu 641 029, India.

*sivarivudevi@gmail.com

ABSTRACT- Nanocrystalline $\text{PbTe}_{100-x}\text{Se}_x$ thin films are prepared using an integrated physical-chemical approach by evaporating chemically synthesized $\text{PbTe}_{100-x}\text{Se}_x$ nanopowders on glass substrates. All the deposited films exhibiting the face centered cubic structure with the crystallite orientation along (200) direction. The crystallite size of the films is within the range 10 - 26 nm. XRD analysis indicated that the lattice constants of $\text{PbTe}_{100-x}\text{Se}_x$ thin films decreased with the increasing amount of Se. Raman spectra of these $\text{PbTe}_{100-x}\text{Se}_x$ thin films show a wavelength shift in the peak position as compared with PbTe due to the addition of Se in PbTe. The observed optical band gap energy in nanocrystalline $\text{PbTe}_{100-x}\text{Se}_x$ films is much larger than the bulk value of 0.32 eV due to quantum confinement effect.

Keywords: PbTe; Doping; X-ray diffraction; Quantum confinement; Optical band gap

1. INTRODUCTION

In the past decades, PbSe and PbTe materials have attracted considerable attention as potential de-vices in thermoelectric (TE) power applications. The performance of a solid-state TE device is greatly determined by the magnitude of the figure-of-merit, ZT, given as $ZT = S^2 T/K$, where S is the Seebeck coefficient or thermoelectric power, σ is the electrical conductivity, K is the thermal conductivity, and T is the absolute temperature of the given TE material. In recent years, significant interest has been directed toward the growth of polycrystalline $\text{PbSe}_{1-x}\text{Te}_x$ and $\text{PbS}_{1-x}\text{Se}_x$ alloy using the quenching method reported by Kumar et al. [1,2]. Ma and Cheng [3] provided the pioneer work on PbSe and $\text{PbSe}_{1-x}\text{S}_x$ (0 \leq x \leq 1.0) thin films using a thermal reduction method. In addition, Dawar et al. [4] showed the effect of hydrogen gas on n-type $\text{Pb}_{0.9}\text{Cd}_{0.1}\text{Te}$ thin

films deposited by flash-evaporation technique, whereas Ahmad et al. [5] showed the morphological crystals of PbSe deposited using CVD technique. To the best of our knowledge, no prior reports have measured the optical properties of a mixture containing PbSe and PbTe, such as $\text{PbTe}_{100-x}\text{Se}_x$ prepared using the integrated physical-chemical approach by evaporating chemically synthesized PbTe nanopowders on glass substrates. In recent years, a growing interest on the composition of $\text{PbTe}_{100-x}\text{Se}_x$ materials has been observed due to their ability to combine the advantages of the two end materials [6]. In the present study, we have prepared nanocrystalline $\text{PbTe}_{100-x}\text{Se}_x$ thin films and studied their performance by XRD, RAMAN, SEM, EDAX and Optical analysis.

2. EXPERIMENTAL

2.1 Preparation of $\text{PbTe}_{100-x}\text{Se}_x$ nanopowders

In this preparation Tellurium (Te, 99.8% (Sigma Aldrich)), Selenium (Se, 99.5% (Sigma Aldrich)), Sodium hydroxide (NaOH, 99% (AR)), NaBH_4 (97.8%, Loba) and lead acetate ($\text{Pb}(\text{CH}_3\text{COO})_2 \cdot 3\text{H}_2\text{O}$, 99% (AR)) were used as the starting materials. In the low-temperature aqueous chemical route, 2M NaOH was dissolved in 200 ml distilled water. The solution was heated to 90° C with continuous stirring. Then 1g of NaBH_4 , 6mmol Te and appropriate amounts of Se were added to get the required stoichiometry $\text{PbTe}_{100-x}\text{Se}_x$ ($0 \leq x \leq 15$). After the color of the solution changed to purple black, 10mmol lead acetate trihydrate powder was added. The solution was then heated for 4 hrs at 110° C and allowed to cool to room temperature at its natural rate. The black powders thus obtained were washed successively with distilled water, acetone and ethanol several times and placed in an oven for 2 hours at 90° C.

2.2 Preparation of nanocrystalline PbTe thin films

$\text{PbTe}_{100-x}\text{Se}_x$ nanopowders prepared by the above mentioned procedure were taken as the source material for thermal evaporation. Using a conventional 12 A4D Hind Hivac Coating unit, $\text{PbTe}_{100-x}\text{Se}_x$ nanopowders were evaporated from a molybdenum boat onto pre cleaned glass substrates. The vacuum chamber is pumped down to 2×10^{-6} mbar. The boat is gradually heated until the material started to evaporate. The vapor molecules leaving the source were deposited onto the substrate surface. The rate of deposition was maintained about 1 Å / Sec and the thickness of the films is monitored by a conventional quartz crystal monitor. The thickness of the prepared nanocrystalline $\text{PbTe}_{100-x}\text{Se}_x$ thin films is 300 nm. The substrates were held at room temperature during the deposition process.

3. RESULTS AND DISCUSSION:

3.1. Structural Analysis

The X-ray diffractograms of nanocrystalline $\text{PbTe}_{100-x}\text{Se}_x$ thin films of different Se composition are shown in Fig.1. The existence of sharp peaks in the diffractogram suggests the polycrystalline nature of the films. For the 15% Se doped PbTe thin films, the peaks at 2θ values 23.015°, 27.779° and 40.241° correspond to (111), (200) and (220) planes of the fcc PbTe lattice respectively.

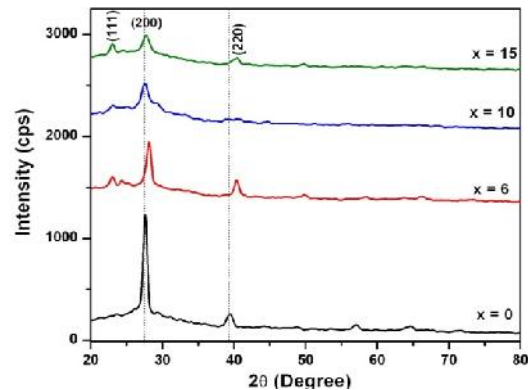


Figure.1. XRD pattern of nanocrystalline $\text{PbTe}_{(100-x)}\text{Se}_x$ thin films

All of the diffraction peaks of nanocrystalline $\text{PbTe}_{100-x}\text{Se}_x$ thin films can be indexed to face centered cubic (fcc) phase of PbTe and it is well matched with standard JCPDS data (Card No: 78-1905). An additional peak at 23.015° corresponds to (111) plane of PbTe appears as the concentration of Se increases. From the XRD, it can be inferred that $\text{PbTe}_{100-x}\text{Se}_x$ films are grown with a preferential orientation along the (200) plane. The absence of any diffraction peaks related to elemental Te, Se or Pb implies the purity of the films. Fig.1 shows that the diffraction peak of the (200) plane shifts to higher angles with increase in Se concentration. This is attributed to the incorporation of Se into the PbTe lattice. This incorporation will lead to an increase in the strain in the lattice which in turn will lead to a decrease in the intensity of the diffraction peaks and an increase in FWHM (full width at half maximum) as the concentration of Se increases.

% of Se Composition (x)	Crystallite Size 'D'(nm)	Strain (ϵ) 10^{-3}	Dislocation density (ρ) lines / m^2	Number of crystallites/unit area	Lattice Constant 'a' (Å)	Volume of the cell $10^{-28} m^3$
0	26.60	1.359	1.19×10^{15}	2.648×10^{15}	6.452	2.685
6	17.217	2.105	2.89×10^{15}	6.010×10^{16}	6.449	2.670
10	13.937	6.910	5.50×10^{16}	2.700×10^{18}	6.433	2.643
15	10.600	10.070	6.51×10^{16}	6.496×10^{18}	6.419	2.548

Table 1. Structural parameters of nanocrystalline PbTe_{100-x}Se_x thin films

The crystallite size (D), dislocation density (ρ), micro-strain (ϵ), lattice constant (a), number of crystallites and the volume of the nanocrystalline PbTe_{100-x}Se_x thin films were calculated and given in the Table 1. The crystallite size of the prepared thin films was estimated and found to be 26.6 - 10.6 nm. It decreases with increasing Selenium concentration. The strain, dislocation density and number of crystallites per unit area increase with rise in Se concentration. Se is smaller in size than Te (ionic radii of Se and Te are 0.184 nm and 0.207 nm respectively) and therefore can easily fit into the Te site. The size mismatch is believed to produce the observed strain. The lattice constant obtained by refinement of XRD data for undoped PbTe thin film is 6.452 Å, which is in good agreement with the standard value (a = 6.454 Å) of bulk fcc PbTe (JCPDS card No.78-1905; Fm3m). The lattice constant (presented in table 1) for nanocrystalline PbTe_{100-x}Se_x thin films decreases with increase in Se concentration and it is smaller than that of undoped PbTe thin film (6.452 Å). The observed crystal lattice compression implies that the inclusion of Se atoms to occupy the substitutional anionic sites in the PbTe lattice. The volume of the cell decreases with increase in Se concentration due to the reduction in the lattice constant.

3.2 Raman spectroscopic Analysis

Raman spectroscopy has been used extensively to study the vibrational properties and electron-phonon coupling. We performed Raman spectroscopy measurements here to investigate how the

compositional variations due to Se doping affect the lattice vibrations and the electron phonon interactions in nanocrystalline thin films. The vibrational properties of lead chalcogenide (PbS, PbSe and PbTe) system have not been fully studied because with its NaCl-type crystal (O_h space group symmetry) structure, where all the atoms at the center of the symmetry, all vibrational modes are Raman inactive [7]. The observation of the first- and second-order Raman peaks on the lead chalcogenides was difficult due to center of inversion which was reported by several groups [8,9]. In spite of this restriction, it may be possible to observe Raman scattering since actual synthesized materials are often not of perfect crystalline structure, especially for thin films. Any deviation from a perfect crystal, such as nonstoichiometry, deformation, dislocations, or extrinsic doping, could cause vibrational modes to be Raman active. Fig. 2 illustrates the Raman spectra of nanocrystalline PbTe_{100-x}Se_x thin films. For undoped PbTe, the mode at 84.87 cm^{-1} is attributed to the transverse optical (TO) phonon mode of TeO₂, which is formed on the PbTe surface [10]. The mode at 559 cm^{-1} is attributed to some species of glass substrate [11]. The mode at 789 cm^{-1} is attributed to lead hydroxide [12]. Se doped PbTe thin films have the modes at 106.41, 115.53 and 119.01 cm^{-1} . These modes are related to excitations of local phonon mode in the vicinity of an impurity atom Se. The observed modes are shifted to higher range with the increase in concentration of Se. This implies that Se enters in the Te sublattice as a substitutional impurity ion. As a consequence a number of Te - ions in PbTe are no longer in the center of inversion symmetry, and PbTe vibrational modes could be Raman active. Thus, the mode at about 106.41 cm^{-1} , the well-known PbTe LO-like mode [13,14], become visible in Raman spectra. This implies that due to doping of Se into PbTe, the Raman modes become active. If the semiconductor (in this case PbTe) is doped with substitutional impurity (Se) i.e., the heavier mass [Te (127.6 g)] is substituted by a lighter impurity [Se (78.96g)], two modes are obtained : a local

mode situated above the optical band, and a gap mode situated above the acoustic band, but below the optical band of the host lattice.

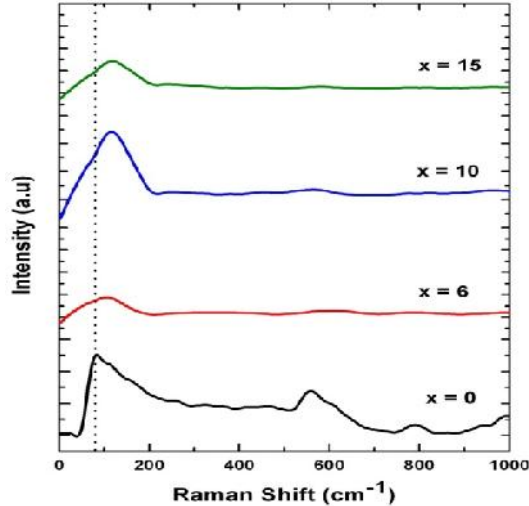


Figure.2 Raman Spectra of nanocrystalline PbTe(100-x)Se_x thin films

In our case, the additional mode has frequencies over the optical range of PbTe (104 cm^{-1}) [14]. We have observed a shift in Raman modes of the nanocrystalline $\text{PbTe}_{100-x}\text{Se}_x$ thin films in comparison with that of earlier reports, which may be due to the size effect in nanomaterials [16].

3.3 Morphological and Compositional analysis

Fig.3 (a) shows the SEM image of nanocrystalline $\text{PbTe}_{100-x}\text{Se}_x$ thin films with $x = 0, 6, 10$ and 15 . It is observed that the undoped PbTe film has spherical particles dispensed throughout the surface and their size is not uniform. Fig.3 (b) depicts the SEM image of the film of 6% Se doped PbTe film. It clearly shows that the film is smooth, homogeneous, fine grained spherical particles of uniform size and well covered to the substrate. Fig.3 (c) shows the SEM image of 10% Se doped PbTe thin film which clearly implies that a stack of parallel aligned rods. From the SEM image, we infer that the one end of the rod is joined to another end of the rod. For the film of 15% Se doped PbTe, we have observed fine grained spherical particles distributed throughout the surface and their size is uniform.

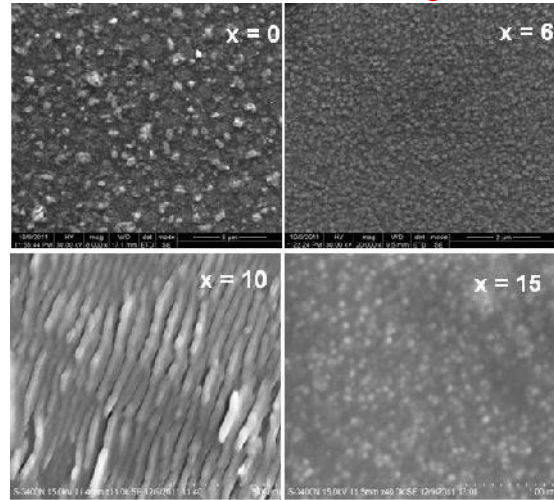


Figure.3 SEM image of nanocrystalline PbTe (100-x)Se_x thin films

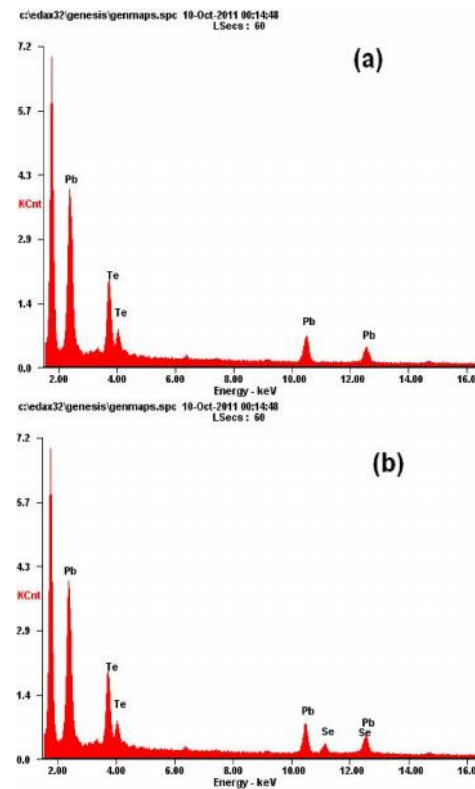


Figure.4. EDAX spectrum of nanocrystalline PbTe(100-x)Se_x thin films with (a) $x = 0$ and (b) $x = 15$

The effect of Te content on the morphology of polycrystalline films is clearly evident in Fig. 3. Similar result has been observed for $\text{PbSe}_{1-x}\text{Te}_x$ thin films. Fig.4. illustrates the EDAX spectrum of undoped and doped PbTe thin films. It is clear from the figures that the presence of Pb, Te and Se is evident from the peaks

marked in the respective EDAX patterns. The peak at less than 2 KeV corresponds to Silicon which is due to the glass substrate used for the preparation of thin film.

3.4 Optical Analysis

The transmittance spectra of the nanocrystalline $PbTe_{100-x}Se_x$ thin films of different concentration of Se are shown in Fig. 5. The transmission spectra show that the transmittance of the films decreases with increase in Se concentration. The maximum transmittance is observed at 2245, 2396, 2066 and 1981nm for $PbTe_{100-x}Se_x$ thin films with x

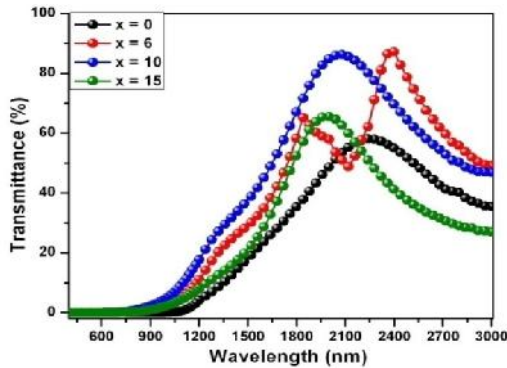


Figure.5 Transmittance spectra of the nanocrystalline $PbTe_{100-x}Se_x$ thin films

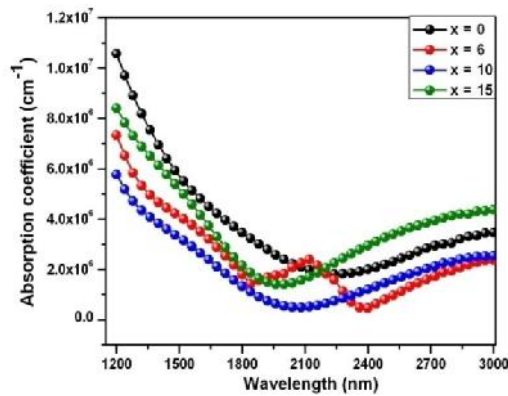


Figure.6 Wavelength dependence of absorbance coefficient of nanocrystalline $PbTe_{100-x}Se_x$ thin films= 0, 6, 10 and 15.

The wavelength at which the maximum transmittance observed is decreased with the increase in Se concentration and the percentage of transmittance also decreased with respect to Se concentration.

Fig. 6. illustrates the wavelength dependence of absorption coefficient () of

nanocrystalline $PbTe_{100-x}Se_x$ thin films of different concentration of Se. The value of decreases with increase in wavelength, reaches minimum then starts to increase with wavelength. It has been found that the absorption coefficient decreased compared with undoped $PbTe$ thin film. With increasing the Selenium concentration bond breaking and bond arrangement can take place, which result in a change in the local structure of the thin films. These include subtle effects such as shifts in the absorption edge, and more substantial atomic and molecular reconfiguration which is associated with changes in absorption coefficient and absorption edge shift.

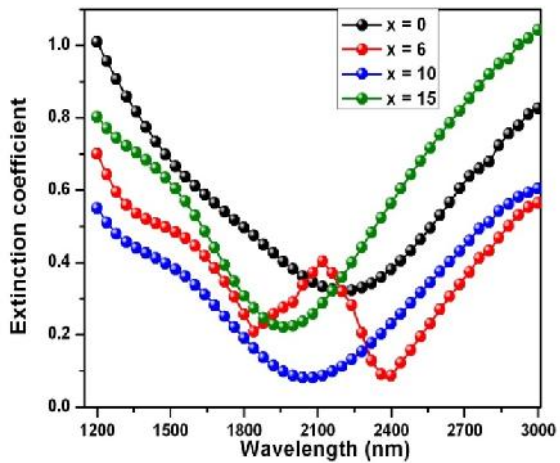


Figure.7. Extinction coefficient versus wave length

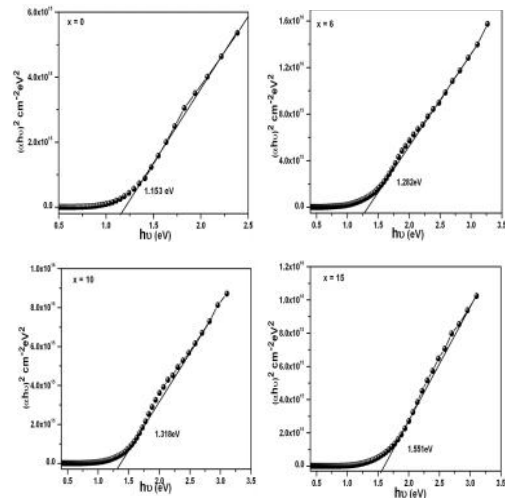


Figure. 8 Tauc plot of $(h\nu)^2$ versus $h\nu$ showing the estimation of direct band gap energy

The extinction coefficient is related to the decay of the amplitude of oscillations of the electric field as the wave penetrated the medium. Extinction coefficient versus wavelength spectra is presented in Fig.7. The value of Extinction coefficient decreases with increase in wavelength, reaches minimum then starts increases for all the films. The extinction coefficient of Se doped PbTe thin films decreased with undoped PbTe film.

From the $(h\nu)^2$ versus $h\nu$ plots presented in Fig.8., the direct band gap of the samples of nanocrystalline $\text{PbTe}_{100-x}\text{Se}_x$ thin films of different concentration of Se were determined. The band gap is estimated by extrapolating the linear portion to the energy axis and is found to be 1.153, 1.282, 1.318 and 1.551 eV for the thin films of different Se concentration. It is worth pointing out that the observed optical band gap energy in nanocrystalline $\text{PbTe}_{100-x}\text{Se}_x$ films is much larger than the bulk value of 0.32 eV due to quantum confinement effect. From XRD results, the grain size of the film is in the range of 10.6 to 26.6 nm, much smaller than the exciton Bohr radius of 150 nm in PbTe. Therefore, the $\text{PbTe}_{100-x}\text{Se}_x$ nanocrystallites in the films can lead to a strong quantum confinement effect, which may account for the optical band gap energy increase.

CONCLUSION

Nanostructured $\text{PbTe}_{100-x}\text{Se}_x$ thin films were prepared by an integrated physical-chemical method. $\text{PbTe}_{100-x}\text{Se}_x$ films of different composition of Se are polycrystalline in nature and the crystallites are grown with a preferential orientation along the (200) plane. Morphology of the films varies as a function of composition of Se. Analysis of the optical absorption data shows that the direct transitions predominates and the values of energy gap are found to vary from 1.153 to 1.551 eV for the thin films of different Se concentration. The absorption coefficient and extinction coefficient are observed to be composition dependent.

REFERENCES

- [1] S. Kumar, M. Hussian, T.P. Sharma, M. Husian, Characterization of $\text{PbSe}_{1-x}\text{Te}_x$ thin films, *J. Phys. Chem. Solids* 64 (2003) 367–376.
- [2] S. Kumar, M.A. Majeed Khan, Shamshad A. Khan, M. Husain, Studies on vacuum evaporated $\text{PbS}_{1-x}\text{Se}_x$ thin films, *Opt. Mater.* 25 (2004) 25–32.
- [3] D.W. Ma, C. Cheng, Preparations and characterizations of polycrystalline PbSe thin films by a thermal reduction method, *J. Alloys Compd.* 509 (2011) 6595–6598.
- [4] A.L. Dawar, C. Jagadish, K.V. Ferdinand, P. Kumar, P.C. Mathur, The effect of hydrogen on the electrical properties of n-type $\text{Pb}_{0.9}\text{Cd}_{0.1}\text{Te}$ thin films, *J. Phys. Chem. Solids* 44 (1983) 453–455.
- [5] K. Ahmad, M. Afzaal, P.O. Brien, G. Hua, J.D. Woollins, Morphological evolution of PbSe crystals via the CVD route, *Chem. Mater.* 22 (2010) 4619–4624.
- [6] X. Xiaochuan, C. Lidong, W. Chunfen, Y. Qin, F. Chude, Template synthesis of heterostructured polyaniline/ Bi_2Te_3 nanowires, *J. Solid State Chem.* 178 (2005) 2163–2166
- [7] J. R. Ferraro, “Factor Group Analysis for Some Common Minerals”, *Applied Spectroscopy* 29, (1975) 418-421.
- [8] T. Shimada, K. L. I. Kobayashi, Y. Katayama, and K. F. Komatsubara, Soft-Phonon-Induced Raman Scattering in IV-VI Compounds *Phys. Rev. Lett.* 39, 143-146 (1977).
- [9] J. G. Shapter, M. H. Brooker, and W. M. Skinner, “Observation of the Oxidation of PbS using Raman Spectroscopy”, *International Journal of Mineral Processing*, 60, (2000) 199-211.
- [10] H.Wu, C.Cao, J.Si, T.Xu, H.Zhang, H.Wu, “Observation of phonon modes in epitaxial PbTe films grown by molecular beam epitaxy” *Journal of Applied Physics*, 101 (2007)103505.
- [11] J. Shang, W. Yao, Y. Zhu, N. Wu, “Structure and photocatalytic performances of glass/ $\text{SnO}_2/\text{TiO}_2$ interface composite film”, *Applied Catalysis A: General*, 257 (2004) 25–32.

[12] V.F. Markov, N.A. Tretyakova, L.N. Maskaeva, V.M. Bakanov, "Hydrochemical synthesis, structure, semiconductor properties of films of substitutional $Pb_{1-x}Sn_xSe$ solid solutions", *Thin Solid Films* 520 (2012) 5227–5231.

[13] Y.I.Ravich, B.A. Efimiva, I.A. Smirov, in: L.S. Stibans (Ed.), *Semiconducting Lead Chalcogenides*, Plenum, New York, 1970.

[14] A.J. Sievers, *Far-Infrared Spectroscopy* (1971) Ed. K.D. Moller, W.G. Rothschild (New York: Wiley) pp.525.

[15] N. Romcevic, A. Golubovic, M. Romcevic, J. Trajic, "Raman spectra of $Pb_{1-x}Mn_xTe$ alloys", *Journal of Alloys and Compounds*, 402 (2005) 36 – 41.

[16] M.S. Niasari, M. Bazarganipour, F. Davar, A.A. Fazl, "Simple routes to synthesis and characterization of nanosized tin telluride compounds", *Applied Surface Science* 257 (2010) 781 – 785.